

High-Rate Synthesis of Cu-BTC Metal-Organic Frameworks

The Faculty of Oregon State University has made this article openly available.
Please share how this access benefits you. Your story matters.

Citation	Kim, K. J., Li, Y. J., Kreider, P. B., Chang, C. H., Wannemacher, N., Thallapally, P. K., & Ahn, H. G. (2013). High-rate synthesis of Cu-BTC metal-organic frameworks. <i>Chemical Communications (Cambridge, England)</i> , 49(98), 11518-11520. doi:10.1039/c3cc46049e
DOI	10.1039/c3cc46049e
Publisher	Royal Society of Chemistry
Version	Accepted Manuscript
Terms of Use	http://cdss.library.oregonstate.edu/sa-termsfuse

Cite this: DOI: 10.1039/c0xx00000x

www.rsc.org/xxxxxx

ARTICLE TYPE

High-Rate Synthesis of Cu-BTC Metal-Organic Frameworks[†]Ki-Joong Kim,^{a,b,†} Yong Jun Li,^{a,b,†} Peter B. Kreider,^a Chih-Hung Chang,^{*a,b} Nick Wannemacher,^a Praveen K. Thallapally,^c and Ho-Geun Ahn^d

Received (in XXX, XXX) Xth XXXXXXXXXX 20XX, Accepted Xth XXXXXXXXXX 20XX

DOI: 10.1039/b000000x

The reaction conditions for the synthesis of Cu-BTC (BTC = benzene-1,3,5-tricarboxylic acid) were elucidated using a continuous-flow microreactor-assisted solvothermal system to achieve crystal size and phase control. A high-rate synthesis of Cu-BTC metal-organic frameworks with BET surface area of more than 1600 m²/g (Langmuir surface area of more than 2000 m²/g) and with a 97% production yield could be achieved with a total reaction time of 5 minutes.

Metal Organic Framework (MOF) materials composed of metal ions, or clusters, as a center and organic molecule ligands as linkers have recently received much attention due to their excellent properties for gas purification, separation, and hydrogen storage.¹ Several hundred different types of MOF materials have been synthesized using a concept known as reticular design.² MOF materials are typically synthesized utilizing batch solvothermal conditions.³ The major drawback is that the reaction under batch solvothermal conditions typically requires long reaction times, sometimes up to several days, depending upon the particular synthesis and/or the reaction conditions such as solvent, temperature, and concentration.⁴ In order to reduce the reaction time from days to minutes, ultrasound,⁵ microwave^{4,6} and mechanochemical⁷ synthesis methods have been developed. The introduction of high-rate methods incorporating solvothermal synthesis has been particularly challenging; additionally the production of MOF materials is not easily scaled up due to equipment limitations associated with batch processing. Thus, the ability to produce high quality MOF with high-throughput is a key step.⁸ A few recent reports have demonstrated unique approaches to reach this goal. Ameloot *et al.*^{9a} synthesized uniform hollow Cu-BTC micro-spheres via interfacial reaction conditions using a continuous droplet microreactor. Gimeno-Fabra *et al.*^{9b} also reported an impressive high-rate synthesis of Cu-BTC via uniform mixing of the reactant streams by using a continuous impinging jet reactor at high pressure. Carné-Sánchez *et al.*^{9c} used a specialized nozzle to spray precursor solutions to create atomized droplets which instantly react to form hollow nanocrystalline MOF in a continuous process.

Herein, we demonstrate the utility of a continuous-flow microreactor-assisted (CFMA) solution-process (Fig. 1 and photograph shown in Fig. S1, ESI[†]) and its ability to control the physical properties (i.e. sizes, morphologies, and porosity) of MOF materials. The CFMA process allows rapid synthesis by inducing crystallization through efficient mixing of the reactant

streams and offers the possibility of controlling the reaction rates by precise control of reaction temperature and residence time. It also provides a convenient platform to elucidate the reaction conditions for the syntheses. A Cu-BTC complex (BTC = benzene-1,3,5-tricarboxylate), consisting of Cu²⁺ ions and BTC linkers, was chosen as a candidate material. Various Cu-BTC complexes have been studied, including Cu₃(BTC)₂·3H₂O,¹⁰ Cu₂(OH)(BTC)(H₂O)·2nH₂O,^{6c,11} and Cu(BTC-H₂)₂(H₂O)₂·3H₂O.¹² Among these phases, Cu₃(BTC)₂·3H₂O (also known as HKUST-1) is particularly favored because of its large surface area, high pore volume, and high chemical stability.^{6c} Cu-BTC compounds were synthesized mainly by conventional hydrothermal processes using long reaction times at relatively high temperatures, and more recently by a number of novel continuous flow processes.⁹ The Cu₃(BTC)₂·3H₂O was successfully synthesized using a CFMA system in an extremely short period of time and lower reaction temperature when compared to those reported in literature.^{10,11} In addition, we demonstrate the synthesis of Cu₂(OH)(BTC)(H₂O)·2H₂O by changing the solvent in the precursors. The reaction conditions for the batch (Brxn) and continuous (Crxn) methods used in the synthesis of Cu-BTC are summarized in Table S1 (ESI[†]).

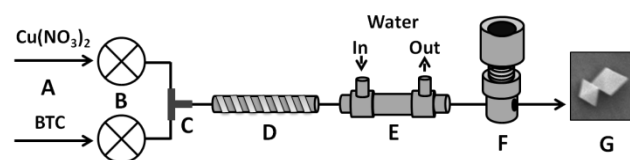


Fig. 1 Schematic diagram of the CFMA system used for the high-rate synthesis of Cu-BTC MOF. (A) Precursors in solutions, (B) HPLC pumps, (C) Mixing zone, (D) Reaction zone, (E) Cooling zone, (F) Back-pressure regulator, and (G) Collecting zone.

In a typical synthesis, the Cu(NO₃)₂ and BTC solutions were continuously pumped (equal volume) into a micro T-mixer (0.75 mm bore) for instantaneous mixing. The reaction was then carried out in a micro-tubular reactor maintained at the desired reaction temperatures; which is then rapidly quenched in a cooler and collected after a manual back pressure regulator (maintained at 100 bar). The production yield of the Brxn and Crxn4 samples were estimated from the consumption of the Cu and were 94% and 97%, respectively. Cu-BTC powder (Crxn4 showing the highest surface area) was obtained at a rate of ~ 2.04 g h⁻¹ via this single channel CFMA system. Higher production rates could be achieved by scaling up the current system by using a

multichannel reactor.¹³

Fig. 2 shows the powder X-ray diffraction (PXRD) patterns of the samples synthesized by Brxn and Crxn methods, where water/ethanol (Brxn & Crxn1), water only (Crxn2) and ethanol only (Crxn3, 4, & 5) were used as the solvents in the $\text{Cu}(\text{NO}_3)_2$ solutions (see Table S1, ESI[†], for complete reaction conditions). The Brxn and Crxn1 sample characteristics (Fig. 2) are in very good agreement with the simulated pattern of $\text{Cu}_3(\text{BTC})_2 \cdot 3\text{H}_2\text{O}$ reported by Klimakow *et al.*^{7b} and Guerrero *et al.*¹⁴. There is no indication of any differences in the crystal structure between batch and continuous synthesis methods, indicating that the synthesis of Cu-BTC is achieved in as short as 5 min via the CFMA system. A comparison of the Raman spectra (Fig. S2, ESI[†]) also verifies similar organic bonding characteristics for the Brxn and Crxn samples.

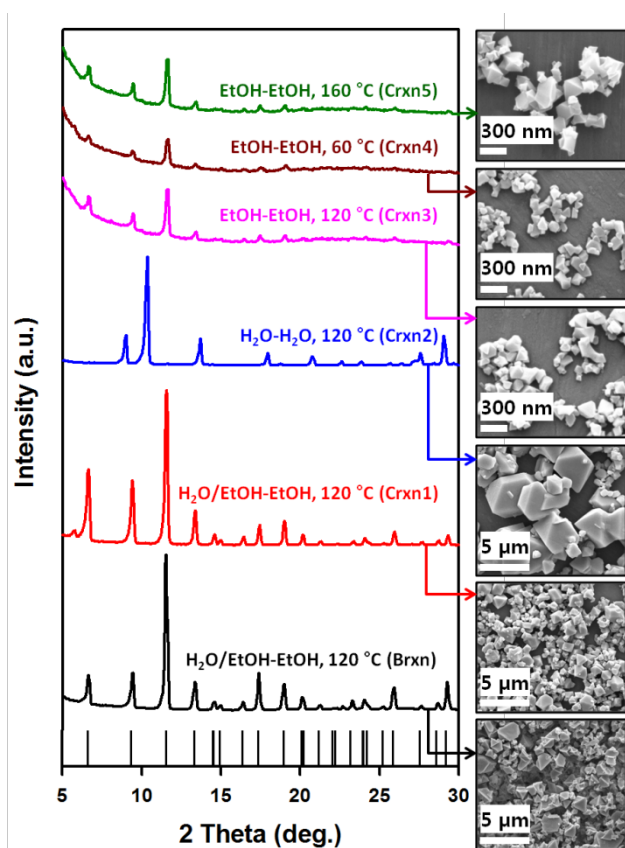


Fig. 2 PXRD patterns of the samples synthesized using different reaction conditions used in the batch and CFMA system. The XRD fingerprint for $\text{Cu}_3(\text{BTC})_2 \cdot 3\text{H}_2\text{O}$, calculated from the crystal structure, is shown for reference. Inserts show the corresponding SEM images.

The PXRD patterns reveal that the reaction in pure water (Crxn2) yields a different phase, which can be assigned to $\text{Cu}_2\text{OH}(\text{BTC})(\text{H}_2\text{O})_n \cdot 2n\text{H}_2\text{O}$,^{6c,11} indicating that the phase of Cu-BTC is strongly dependent on the solvent used in the precursor solutions.

The effects of $\text{Cu}(\text{NO}_3)_2$ solution solvents on the morphology and particle size of the samples synthesized via the CFMA system were also investigated using SEM images (insert of Fig. 2). It can be seen that different sizes of Cu-BTC particles are formed with a mixture of cubic and octahedral shapes. Synthesis in water produces larger particles that vary in size from 2 to 4 μm ,

whereas the sample synthesized in ethanol shows more uniform shaped smaller particles (~ 150 nm). In general, the particles decreased in size when ethanol was used in the $\text{Cu}(\text{NO}_3)_2$ solutions, which is in good agreement with the other results.¹⁵

Samples from Crxn3, Crxn4, and Crxn5 demonstrate that increasing the synthesis temperature results in the average particle size changing from ~ 100 nm for 60 °C to ~ 250 nm for 160 °C (insert of Fig. 2), indicating that larger Cu-BTC crystals are formed with increasing reaction temperature. SEM images also confirmed that the crystals formed well at all tested reaction temperatures, indicating the thermal stability of the synthesized Cu-BTC materials. Thermogravimetric analysis shows that the samples are thermally stable up to 330 °C (Fig. S3, ESI[†]).

Fig. 3A shows the N_2 gas adsorption/desorption isotherms (further details shown in Fig. S4, ESI[†]). According to the IUPAC classification,¹⁶ Brxn shows a typical isotherm of Type I and a very small and wide hysteresis loop at $P/P_0 = 0.5$ to 0.9. Interestingly, Crxn samples yielded an isotherm which can be most closely classified as a combination of Type I and IV with a negligible hysteresis loop upon desorption of the gas from the pores. To our knowledge, this particular isotherm shape for the Cu-BTC MOFs has not been reported previously. The vertical nature of the N_2 adsorption isotherms at low pressures indicates that the size of micropores is extremely uniform, being a main characteristic of MOF solids. Furthermore, a “tail” in the very narrow range of $P/P_0 = 0.95$ to 1.0 suggests a slight characteristic of Type IV isotherms, indicating the existence of some large macropores, most probably from intra-agglomerate voids in the sample. The logarithmic isotherm of the Crxn4 sample is shown in Fig. S5 (ESI[†]), where distinct regions can be observed. The Crxn4 sample has a much larger BET surface area (S_{BET}), micropore volume (V_{micro}) and total pore volume (V_{total}) than other Crxn samples (Table S2, ESI[†]). Physisorption measurements of the Crxn4 sample yield a S_{BET} of $1673 \text{ m}^2 \text{ g}^{-1}$ (Langmuir surface area of $2021 \text{ m}^2 \text{ g}^{-1}$) and V_{total} of $0.714 \text{ cm}^3 \text{ g}^{-1}$. The V_{total} of Crxn4 in this study ($0.714 \text{ cm}^3 \text{ g}^{-1}$) is close to the results found by Xiang *et al.*^{17a} ($0.730 \text{ cm}^3 \text{ g}^{-1}$) and Chowdhury *et al.*^{17b} ($0.753 \text{ cm}^3 \text{ g}^{-1}$). The SEM and S_{BET} data suggest that the surface area increased with decreasing particle size. In general, one would not expect such size dependency for highly porous MOFs. One possible explanation for this observed correlation might be attributed to mass transport limitations during the activation process (i.e. the smaller particles experience higher activation process efficiency).

Pore size distributions can be calculated very precisely with DFT models, especially for micropores with pore diameter less than 2 nm,¹⁸ and the results of the evaluation for Crxn4 are shown in Fig. 3B. The bimodal micropore structure was confirmed at ~ 0.9 nm and at below ~ 0.35 nm - these results are in excellent agreement with the crystallographic structure for the main channels and the tetrahedral side pockets of Cu-BTC (space group $Fm\text{-}3m$), respectively. Furthermore, the Cu-BTC material is mostly microporous (< 1 nm) with about 90% of V_{total} being attributed to V_{micro} (Table S2, ESI[†]).

In summary, Cu-BTC with a highly-developed microporous network (< 1 nm pore size) and with S_{BET} of $1673 \text{ m}^2 \text{ g}^{-1}$ was rapidly synthesized within 5 min. The particle size and crystal phase of these materials can be adjusted by changing the relative

ratios of water and ethanol solvents in the $\text{Cu}(\text{NO}_3)_2$ solution used as precursor. In general, the lower reaction temperatures correspond to a decrease in particle size and an increase in total pore volume and surface area. We believe that the new continuous synthetic method can be extended to the production of other highly porous metal-organic frameworks.

This work was funded by the US Department of Energy, Industrial Technologies Program through award #NT08847, under contract DE-AC-05-RL01830, DOE-ARPA-E Navy and ONAMI matching grants. Oregon Process Innovation Center is supported by Oregon BEST equipment grants.

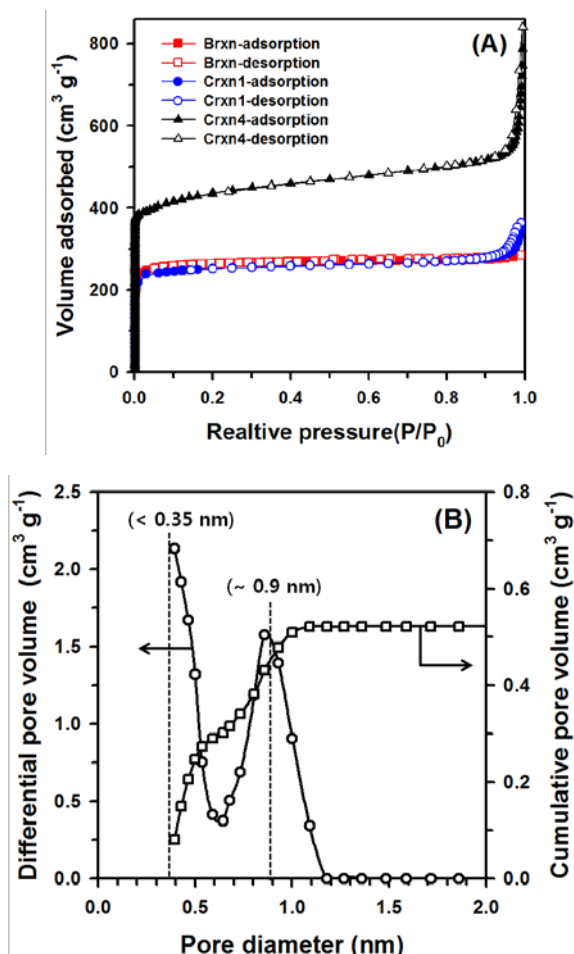


Fig. 3 (A) N_2 gas isotherms from the Brxn, Crxn1 and Crxn4 samples. (B) Pore size distributions obtained by DFT method and the cumulative pore size distribution of Crxn4 sample.

Notes and references

^a School of Chemical, Biological & Environmental Engineering, Oregon State University, Corvallis, OR 97331, United States. E-mail: chih-hung.chang@oregonstate.edu

^b Oregon Process Innovation Center, Microproducts Breakthrough Institute, Corvallis, OR 97330, United States

^c Pacific Northwest National Laboratory, Richland, WA 99352, United States

^d Department of Chemical Engineering, Suncheon National University, Suncheon, Jeonnam 540-742, South Korea

† Electronic supplementary information (ESI) available: Experimental details on Cu-BTC synthesis and characterization. Further Raman, TGA and N_2 gas adsorption-desorption results.

‡ These authors contributed equally to this work.

- (a) H. K. Chae, D. Y. Siberio-Perez, J. Kim, Y. B. Go, M. Eddaoudi, A. J. Matzger, M. O’Keeffe and O. M. Yaghi, *Nature*, 2004, **427**, 523-527; (b) S. J. Dalgarno, P. K. Thallapally, L. J. Barbour and J. L. Atwood, *Chem. Soc. Rev.*, 2007, **36**, 236-245; (c) J. R. Li, R. J. Kuppler and H. C. Zhou, *Chem. Soc. Rev.*, 2009, **38**, 1477-1504; (d) H. Furukawa, N. Ko, Y. B. Go, N. Aratani, S. B. Choi, E. Choi, A. O. Yazaydin, R. Q. Snurr, M. O’Keeffe, J. Kim and O. M. Yaghi, *Science*, 2010, **329**, 424-428; (e) O. Shekhah, J. Liu, R. A. Fischer and C. Woll, *Chem. Soc. Rev.*, 2011, **40**, 1081-1106; (f) J. A. Bohman and M. A. Carreon, *Chem. Commun.*, 2012, **48**, 5130-5132; (g) P. Nugent, Y. Belmabkhout, S. D. Burd, A. J. Cairns, R. Luebke, K. Forrest, T. Pham, S. Ma, B. Space, L. Wojtas, M. Eddaoudi and M. J. Zaworotko, *Nature*, 2013, **495**, 80-84.
- O. M. Yaghi and M. O’Keeffe, *J. Solid State Chem.*, 2000, **152**, 1-2.
- (a) H. Li, M. Eddaoudi, M. O’Keeffe and O. M. Yaghi, *Nature*, 1999, **402**, 276-278; (b) G. Ferey, *Chem. Soc. Rev.*, 2008, **37**, 191-214; (c) J. A. Martens, J. Jammaer, S. Bajpe, A. Aerts and Y. Lorgouilloux, *Microporo. Mesoporo. Mater.*, 2011, **140**, 2-8.
- M. Schlesinger, S. Schulze, M. Hietschold and M. Mehning, *Microporo. Mesoporo. Mater.*, 2010, **132**, 121-127.
- (a) W. J. Son, J. Kim and W. S. Ahn, *Chem. Commun.*, 2008, 6336-6338; (b) Z.-Q. Li, L.-G. Qiu, T. Xu, Y. Wu, W. Wang, Z.-Y. Wu and X. Jiang, *Mater. Lett.*, 2009, **63**, 78-80; (c) J.-D. Xiao, L.-G. Qiu, F. Ke, Y.-P. Yuan, G.-S. Xu, Y.-M. Wang and X. Jiang, *J. Mater. Chem. A*, 2013, **1**, 8745-8752.
- (a) Y. Yoo and H. K. Jeong, *Chem. Commun.*, 2008, 2441-2443; (b) N. A. Khan and S. H. Jhung, *Bull. Korean Chem. Soc.*, 2009, **30**, 2921-2926; (c) Y. K. Seo, G. Hundal, I. T. Jang, Y. K. Hwang, C. H. Jun and J.-S. Chang, *Microporo. Mesoporo. Mater.*, 2009, **119**, 331-337; (d) S. Diring, S. Furukawa, Y. Takashima, T. Tsuruoka and S. Kitagawa, *Chem. Mater.*, 2010, **22**, 4531-4538; (e) N. A. Khan, E. Haque and S. H. Jhung, *Phys. Chem. Chem. Phys.*, 2010, **12**, 2625-2631.
- (a) W. Yuan, A. L. Garay, A. Pichon, R. Clowes, C. D. Wood, A. I. Cooper and S. L. James, *Cryst. Eng. Comm.*, 2010, **12**, 4063-4065; (b) M. Klimakow, P. Klobes, A. F. Thunemann, K. Rademann and F. Emmerring, *Chem. Mater.*, 2010, **22**, 5216-5221; (c) B. P. Biswal, S. Chandra, S. Kandambeth, B. Lukose, T. Heine and R. Banerjee, *J. Am. Chem. Soc.*, 2013, **135**, 5328-5331.
- G. Ferey, *Chem. Soc. Rev.*, 2008, **37**, 191-214.
- (a) R. Ameloot, F. Vermoortele, W. Vanhove, M. B. J. Roeffaers, B. F. Sels and D. E. De Vos, *Nature Chem.*, 2011, **3**, 382-387; (b) M. Gimeno-Fabra, A. S. Munn, L. A. Stevens, T. C. Drage, D. M. Grant, R. J. Kashtiban, J. Sloan, E. Lester and R. I. Walton, *Chem. Commun.*, 2012, **48**, 10642-10644; (c) A. Carné-Sánchez, I. Imaz, M. Cano-Sarabia and D. Maspoch, *Nature Chem.*, 2013, **5**, 203-211.
- (a) J. Gascon, S. Aguado and F. Kapteijn, *Microporo. Mesoporo. Mater.*, 2008, **113**, 132-138; (b) D. Mustafa, E. Breynaert, S. R. Bajpe, J. A. Martens and C. E. A. Kirschhock, *Chem. Commun.*, 2011, **47**, 8037-8039.
- J. Chen, T. Yu, H. Xiao, G. Zhou, L. Weng, B. Tu and D. Zhao, *Chem. Lett.*, 2003, **32**, 590-591.
- Y. Mao, L. Shi, H. Huang, Q. Yu, Z. Ye and X. Peng, *Cryst. Eng. Comm.*, 2013, **15**, 265-270.
- H. D. Jin, A. Garrison, T. Tseng, B. K. Paul and C. H. Chang, *Nanotechnology*, 2010, **21**, 445604.
- V. V. Guerrero, Y. Yoo, M. C. McCarthy and H. K. Jeong, *J. Mater. Chem.*, 2010, **20**, 3938-3943.
- L. H. Wee, M. R. Lohe, N. Janssens, S. Kaskel and J. A. Martens, *J. Mater. Chem.*, 2012, **22**, 13742-13746.
- (a) S. Brunauer, L. S. Deming, W. E. Deming and E. Teller, *J. Am. Chem. Soc.*, 1940, **62**, 1723-1732; (b) S. Kitagawa, R. Kitaura and S. Noro, *Angew. Chem. Int. Ed.*, 2004, **43**, 2334-2375.
- (a) P. Chowdhury, C. Bikkina, D. Meister, F. Dreisbach and S. Gumma, *Microporo. Mesoporo. Mater.*, 2009, **117**, 406-413; (b) Z. Xiang, Z. Hu, D. Cao, W. Yang, J. Lu, B. Han and W. Wang, *Angew. Chem. Int. Ed.*, 2011, **50**, 491-494.
- C. Lastoskie, K. E. Gubbins and N. Quirke, *J. Phys. Chem.*, 1993, **97**, 4786-4796.